Acta Cryst. (1986). B42, 51-55

Refinement of the Structure of Deuterated Nickel Hydroxide, $Ni(OD)_2$, by Powder Neutron Diffraction and Evidence for Structural Disorder in Samples with High Surface Area

BY C. GREAVES AND M. A. THOMAS

Department of Chemistry, University of Birmingham, Birmingham B15 2TT, England

(*Received* 30 *May* 1985; *accepted* 5 *September* 1985)

Abstract

The structure of deuterated nickel hydroxide (H/D *ca* 0·1), prepared using hydrothermal techniques, has been refined using fixed-wavelength ($\lambda = 1{\cdot}386$ Å) powder neutron diffraction data collected at 298 K: $M_r = 94{\cdot}74$ [$Ni(OD)_2$], trigonal, $P\bar{3}m1$, $a = 3.126$ (1), $c = 4{\cdot}593$ (1) Å, $V = 38{\cdot}87$ (4) Å^3, $Z = 1$, $D_x = 4{\cdot}05$ g cm^{-3} [$Ni(OD)_2$]. Rietveld refinement ($R_{wp} = 0{\cdot}069$, $R_{exp} = 0{\cdot}025$) indicates anisotropic D vibrations similar to those observed for $Ca(OH)_2$ and $Mg(OH)_2$ and after correction for thermal motion an O–D distance of 0·973 (4) Å is obtained. Data from a high-surface-area $Ni(OH)_2$ sample show additional weak peaks which are attributed to the presence of H_2O defects; such a model is shown to be consistent with the observed infrared spectrum.

Introduction

Most secondary alkaline cells contain $Ni(OH)_2$ cathodes at which reversible oxidation to nickel(III) or even nickel(IV) oxide hydroxides occurs; for simplicity, the oxidized phases may be represented as NiOOH. These transformations require solid-state proton migration, but their study has been hindered by the lack of reliable structural information for the relevant phases, due principally to difficulties in obtaining highly crystalline samples. For example, although conversion of $Ni(OH)_2$ to β-NiOOH (the simplest oxidized phase from a chemical stoichometry viewpoint) involves H abstraction from the CdI_2 layer structure of $Ni(OH)_2$, details of the consequential Ni- and O-atom rearrangements are unknown and various structure types have been suggested (Tuomi, 1965; Kober, 1967; McEwen, 1971; Oliva *et al.*, 1982). The hydroxides of many divalent metals, *e.g.* Mg, Ca, Co, Cd, have similar structures to $Ni(OH)_2$ (trigonal, $P\bar{3}m1$, for which the z coordinates of O and H are the only structural variables), but precise structural determinations affording reliable H-atom positions are sparse. The most comprehensive study was a single-crystal neutron diffraction examination of $Ca(OH)_2$ (Busing & Levy, 1957), for which a rigorous treatment of the anisotropic H-atom thermal parameters suggested an O–H bond length of 0·983 Å (Busing & Levy, 1964). A neutron diffraction study of $Mg(OH)_2$ (Zigan & Rothbauer, 1967) implied a similar O–H distance of 1·03 Å and confirmed the anisotropic nature of the H thermal ellipsoid. In $Ca(OH)_2$ and $Mg(OH)_2$, the octahedral cation coordination polyhedra are flattened trigonally, along the z axis, resulting in O–M–O angles of 98·5 and 97·0° respectively. Such distortions are in accordance with molecular-orbital calculations (Peterson, Hill & Gibbs, 1979) and the observed angles are in close agreement with the constant distortion of 97·4 ± 0·4°, suggested for all brucite-like hydroxides by the correlation between unit-cell parameters and M–O distances (Brindley & Chih-Chun Kao, 1984). However, a limited powder neutron diffraction data set from $Ni(OH)_2$ (Szytula, Murasik & Balanda, 1971) implied a low flattening angle of 95·1°, a correspondingly large Ni–O distance of 2·12 Å (*cf.* 2·09 Å in NiO) and also an O–H distance of 1·06 Å, which is large for a free OH^- ion. In the light of these apparently anomalous parameters, the infrared absorption spectrum of $Ni(OH)_2$ is of relevance. The OH vibration at *ca* 3640 cm^{-1} is sharp for samples of large crystallite size, as expected for free OH^- ions, but is broadened by a shoulder at *ca* 3400 cm^{-1} for samples with smaller crystallites (Kober, 1965; Sakashita & Sato, 1973; Greaves, Thomas & Turner, 1983), which is more compatible with some hydrogen-bonding interactions. Since the redox properties of $Ni(OH)_2$ electrodes, which clearly relate to proton transport, also depend on crystallite size (Falk & Salkind, 1969; Greaves, Thomas & Turner, 1983), the structure of $Ni(OD)_2$ of large crystallite size has been examined by powder neutron diffraction, and the results compared with data, of necessarily poorer quality, from $Ni(OH)_2$ of small crystallite size.

Experimental and structure refinement

$Ni(OH)_2$ was prepared by precipitation from solutions of BDH AnalaR $NiSO_4.7H_2O$ and KOH. To minimize the effects of incoherent neutron scattering from H, a deuterium-enriched sample was obtained hydrothermally using $NaOD/D_2O$ solution. The materials were contained in a PTFE-lined stainless-

0108-7681/86/010051-05$01.50

steel autoclave which was heated at 423 K under oxygen (200 bar, 2×10^7 Pa) for 16 h. The conditions were chosen to induce crystal growth and effect substitution of H by D. The procedure was repeated several times, and the extent of H/D exchange monitored using the intensities of the antisymmetric OH and OD infrared bands at 3640 and 2680 cm^{-1}. In this way, the final ratio D/(H+D) was estimated to be 0·90 (1), which compares with a value of 0·91 (2) obtained from a mass-spectrometer analysis of the H_2O, D_2O *etc.* peaks following thermal decomposition of the sample. X-ray diffractometer full width at half maximum (FWHM) measurements showed the crystals to be platelets with average thickness 400 (40) Å along [001], and diameter 1800 (200) Å.

Fixed-wavelength [1·386 Å from (117) planes of a germanium monochromator, take-off angle 122°] powder neutron diffraction data were collected at ambient temperature on the *D1A* diffractometer, ILL (Hewat & Bailey, 1976). The sample (*ca* 5 g) was sealed in a 16 mm diameter vanadium can, and data were collected in 24 h for 2θ from 6–158° using 10 counters with a step increment of 0·05°. The data were analysed using a modified Rietveld technique (Reitveld, 1967, 1969) which allows refinement of anisotropic thermal parameters; Ni, O, H and D scattering lengths of 10·3, 5·8, −3·74 and 6·67 (all fm) were used. The background, *b*, was estimated between reflections and elsewhere was determined by linear interpolation. Weights of $250/(y_{obs}+b)$ were assigned to individual profile points, where $(y_{obs}+b)$ represents the total counter intensity. The profile contained 41 resolvable reflections and 16 parameters were refined: the structural variables, including an allowance for anisotropic motion of H/D alone, the H/D occupation parameter, three FWHM parameters, scale factor, and parameters to correct for peak asymmetry [applied below 50° (2θ)], preferred orientation and zero-point effects. The plate-like crystal habit resulted in crystallite size broadening effects which were dependent on scattering vector, and therefore varied significantly from peak to peak.

Table 1. *Refined structural parameters for* $Ni(OD)_2$

Estimated standard deviations (e.s.d.'s) in the last digits are indicated in parentheses. $a = 3{\cdot}126\,(1)$, $c = 4{\cdot}593\,(1)$ Å.

	x	y	z	B_{iso} (Å^2)	Occupation per cell
Ni	0	0	0	0·71 (3)	1·0
O	$\frac{1}{3}$	$\frac{2}{3}$	0·2221 (3)	0·76 (4)	2·0
D	$\frac{1}{3}$	$\frac{2}{3}$	0·4275 (3)	—*	1·80 (2)

Maximum correlations between structural parameters

Occupation (D)–β_{22}	61%
B_{Ni}–B_O	57%
Occupation (D)–β_{11}	54%

* For the thermal parameter $\exp[-(\beta_{11}h^2+\beta_{22}k^2+\beta_{33}l^2+2\beta_{12}hk+2\beta_{13}hl+2\beta_{23}kl)]$, $\beta_{11}=\beta_{22}=2\beta_{12}=0.102(2)$, $\beta_{33}=0.013(1)$, $\beta_{13}=\beta_{23}=0$.

Consequently the refinement was unsatisfactory (weighted profile index $R_{wp}=0{\cdot}141$ compared with the statistically expected value $R_{exp}=0{\cdot}025$), and a modified function for FWHM was introduced which has been described elsewhere (Greaves, 1985). Much better agreement was obtained ($R_{wp}=0{\cdot}085$) and further improvements resulted from the use of a pseudo-Voigt peak-shape function (see, for example, Young & Wiles, 1982) rather than a pure Gaussian. The final agreement factors were $R_{wp}=0{\cdot}069$, $R_p=0{\cdot}081$, $R_B=0{\cdot}029$ where R_p and R_B represent the unweighted profile index and the Bragg index based on deconvoluted peak intensities.* Fig. 1 compares the observed and calculated profiles, and the refined atomic parameters are presented in Table 1. A small correction (equivalent to $\Delta B_{iso}=0{\cdot}14$ Å^2) was applied to the thermal parameters to compensate for absorption effects (Hewat, 1979). A (110) ORTEP diagram (Johnson, 1965) is shown in Fig. 2. The introduction

* A list of observed and calculated intensities for each profile point has been deposited with the British Library Lending Division as Supplementary Publication No. SUP 42440 (12 pp.). Copies may be obtained through The Executive Secretary, International Union of Crystallography, 5 Abbey Square, Chester CH1 2HU, England.

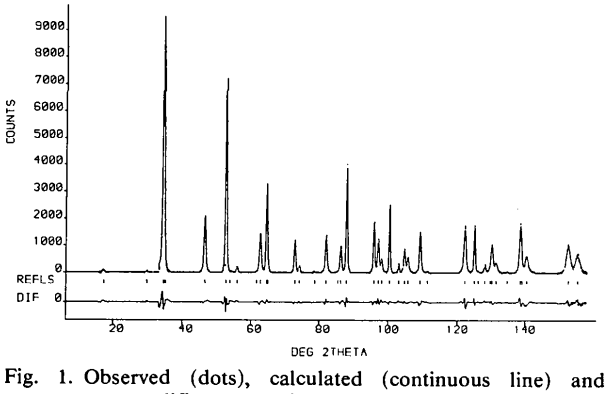

Fig. 1. Observed (dots), calculated (continuous line) and difference profiles for $Ni(OD)_2$.

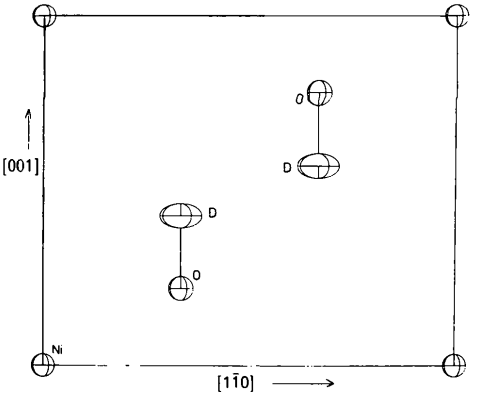

Fig. 2. *ORTEP* diagram of the (110) plane in the $Ni(OD)_2$ unit cell.

of the additional parameter required to describe anisotropic H/D motion was justified by the decrease in R factors relative to those for a purely isotropic model: $R_{wp} = 0{\cdot}078$, $R_p = 0{\cdot}092$, $R_B = 0{\cdot}039$. Although anisotropic motion for Ni and O was considered, no significant changes in agreement indices or temperature factors resulted and, in view of the limited number of reflection intensity data, it was considered appropriate to maintain an isotropic constraint for these atoms.

A sample of $Ni(OH)_2$ which had not been hydrothermally treated was also examined. Preparation of a deuterated sample of this type was unfortunately not possible due to the very large volume of D_2O which would have been required [$Ni(OH)_2$ samples need extensive washing to achieve acceptable SO_4^{2-} impurity levels]. X-ray diffraction FWHM measurements were consistent with a mean crystallite size of 35 (5) × 170 (20) Å and Fig. 3 shows neutron diffraction data obtained on the low-resolution $D2$ diffractometer, step 0·2°, $\lambda = 1{\cdot}219$ Å. Rigorous refinement was clearly impractical from such data, but it is relevant to note the appearance of additional weak peaks (arrowed). The implications of these data are discussed fully below.

Discussion

The neutron diffraction results from $Ni(OD)_2$ confirm the brucite structure. The refined D occupation parameter, reduced below 2·0 by H substitution, implied $D/(H+D) = 0{\cdot}93$ (1), which agrees well with the results of infrared and mass-spectrometry analyses. The positional parameters for O and D, z_O and z_D, are very different from those reported by Szytula, Murasik & Balanda (1971), and determine the bond distances and angles shown in Table 2. The O–D distance calculated using the midpoints of the thermal ellipsoids is seen to be quite short, 0·932 (2) Å, but is consistent with the single-crystal neutron diffraction study of $Ca(OH)_2$ (Busing & Levy, 1957), from which an uncorrected O–H distance of 0·936 (3) Å was deduced. Correction for 'riding' motion of H relative to O increased the distance in $Ca(OH)_2$ to 0·983 (4) Å (Busing & Levy, 1964), and a similar treatment for $Ni(OD)_2$ results in the value 0·973 (3) Å, which is typical for OH^- ions. Comparative data for $Ni(OD)_2$, $Ca(OH)_2$ and $Mg(OH)_2$ are shown in Table 3. It is interesting to note that whereas the thermal parameters imply similar H/D mean-square displacements in all three hydroxides, the smaller unit-cell sizes of $Ni(OD)_2$ and $Mg(OH)_2$ lead to significantly shorter D–D and H–H separations, and indicates the possibility of correlated motion of neighbouring atoms. It is also pertinent that the distortion of the NiO_6 octahedra, indicated by the O–Ni–O angles (Table 2), is precisely that suggested by Brindley & Chih-Chun Kao (1984) for all brucite-like hydroxides.

Although the neutron diffraction data obtained from $Ni(OH)_2$ with high surface area were not suitable for reliable structure refinement, these nevertheless have several important structural implications. The small peaks, arrowed in Fig. 3, do not relate simply to the brucite unit cell and were therefore considered to reflect short-range order associated with some structural defects. The absence of these peaks from X-ray diffraction traces suggested that the disorder primarily involves the H sublattice. The use

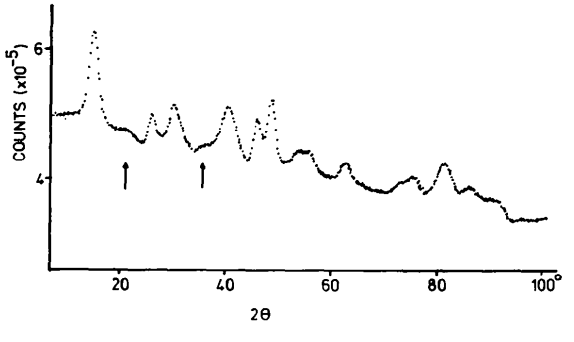

Fig. 3. Neutron diffraction profile for $Ni(OH)_2$.

Table 2. *Selected bond distances* (Å) *and angles* (°)

O–O	[×6]	3·126 (1)	Ni–O	[×6]	2·073 (1)
	[×3]	3·126 (2)	D–D	[×3]	1·923 (2)
	[×3]	2·724 (2)	O–D		0·943 (2)
			O–$D^*_{corrected}$		0·973 (4)
O–Ni–O	[×6]	97·86 (7)			
	[×6]	82·14 (7)			
	[×3]	180·0			

* Corrected for anisotropic motion using the 'riding-motion' approximation (Busing & Levy, 1964): $O\text{–}D_{corrected} = (O\text{–}D) + [2(\langle u_D^2\rangle - \langle u_O^2\rangle))/2(O\text{–}D)]$, where u represents displacements normal to the O–D bond.

Table 3. *Comparison of* $Ca(OH)_2$, $Mg(OH)_2$ *and* $Ni(OD)_2$ *structural parameters*

Parameter	$Ca(OH)_2$ [a]	$Mg(OH)_2$ [b]	$Ni(OD)_2$
a (Å)	3·5918 (3)	3·142 (1)	3·126 (1)
c (Å)	4·9063 (7)	4·766 (2)	4·593 (1)
z_O	0·2341 (3)	0·22167 (7)	0·2221 (3)
$z_{H/D}$	0·4248 (6)	0·4303 (12)	0·4275 (3)
$B_{M,x}$ (Å^2)	0·70 (7)	0·0 (3)	0·71 (3)
$B_{M,z}$ (Å^2)	1·25 (9)	0·27 (18)	0·71 (3)
$B_{O,x}$ (Å^2)	0·73 (5)	0·2 (2)	0·76 (4)
$B_{O,z}$ (Å^2)	0·93 (5)	0·9 (2)	0·76 (4)
$B_{H/D,x}$ (Å^2)	4·23 (14)	2·9 (4)	2·99 (6)
$B_{H/D,z}$ (Å^2)	1·34 (10)	0·9 (2)	1·10 (8)
O–H/D (Å)	0·936 (3)	0·995 (8)	0·943 (2)
$O\text{–}H/D_{corrected}$ (Å)	0·983 (4)	1·03 (1)	0·973 (4)
M–O (Å)	2·371 (1)	2·102 (3)	2·073 (1)
O–O[c] (Å)	3·333 (2)	3·218 (4)	3·126 (2)
H/D–H/D (Å)	2·202 (2)	1·932 (4)	1·923 (2)
O–M–O (°)	98·48 (6)	96·7 (2)	97·86 (7)
O–H/D–O (°)	128·9 (4)	133 (1)	131·7 (3)

Notes: (*a*) Data from Busing & Levy (1957, 1964). (*b*) Data from Zigan & Rothbauer (1967). (*c*) This represents the separation of the O atoms shown in Fig. 2.

of Rietveld analysis to refine the unit cell and non-structural parameters, whilst constraining the structural variables to the values determined for $Ni(OD)_2$, resulted in two significant observations. Firstly, the unit-cell dimensions, $a = 3{\cdot}119\,(4)$ and $c = 4{\cdot}686\,(4)$ Å, show a substantial increase in c relative to that observed for $Ni(OD)_2$. This effect was supported by X-ray diffractometer data, for which correlation of c with crystallite size was also apparent. Secondly, the agreement factors ($R_{wp} = 0{\cdot}183$, $R_B = 0{\cdot}103$, $R_{exp} = 0{\cdot}032$) were unsatisfactory. Although high values of R_{wp} and R_B are to be expected due to the high incoherent background, the inadequacy of the peak-shape function for such broadened peaks and contributions from the short-range-order peaks, additional discrepancies between calculated and observed peak intensities were apparent; in particular, the 001 intensity was significantly higher than expected. Freeing z_O and z_H produced a considerable shift in H alone to $z_H = 0{\cdot}453\,(5)$, with R_{wp} and R_B decreasing to 0·126 and 0·066 respectively. In a recent examination of the dehydration mechanism for $Ca(OD)_2$ (Chaix-Pluchery, Bouillot, Ciosmak, Niepce & Freund, 1983), it was found that at temperatures well below the onset of dehydration, the 001 intensity decreased with temperature more rapidly than other reflection intensities. This was attributed to strain caused by D migration and the conversion of some OD^- sites to O^{2-} and D_2O; this inference has been supported by Raman spectroscopy (Chaix-Pluchery, Ciosmak, Niepce & Peyrard, 1984). Bearing in mind that the scattering length of H is negative, it seems possible that a similar defect model might be responsible for the increased 001 intensity for our $Ni(OH)_2$ sample at ambient temperature. Accordingly, the change in z_H, which implies the large O–H distance of 1·08 Å, similar to that reported by Szytula, Murasik & Balanda (1971), is thought to represent not a unique H site but an average position in a disordered structure containing H_2O and O^{2-} defects. The occurrence of significant concentrations of such defects would also rationalize the unit-cell expansion along z, and, of course, infrared absorption bands relevant to H_2O molecules within the lattice would be expected. In this respect, it is interesting to compare the infrared absorption spectrum of this material with that of $Ni(OH)_2$ of similar crystallite size to the $Ni(OD)_2$ sample, Fig. 4. For the sample of smaller crystallite size, broadening of the antisymmetric OH band and the appearance of a band at about 1600 cm^{-1} are both consistent with the presence of structural H_2O molecules, although strongly adsorbed H_2O could contribute to these bands since complete removal is difficult under normal drying conditions. Similar effects have been observed in $Ca(OH)_2$ and $Mg(OH)_2$ at elevated temperatures (Freund, Gieseke & Nagerl, 1975; Wengeler, Martens & Freund, 1980).

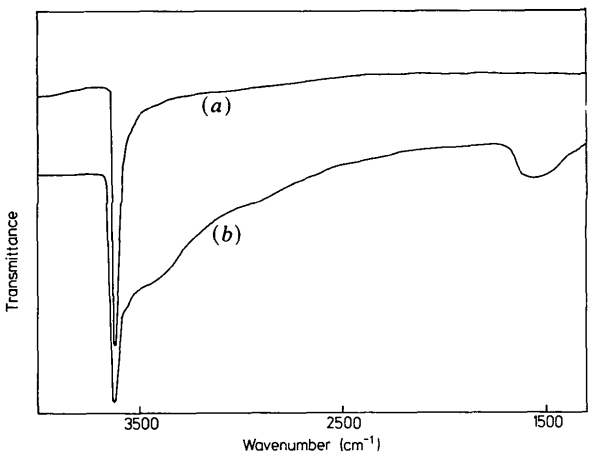

Fig. 4. Infrared spectra of $Ni(OH)_2$ samples with (*a*) large and (*b*) small crystallite sizes.

In the present study, the structural differences between the samples examined are thought to reflect an important influence of surface effects on the bulk defect structure. Indeed, it has been pointed out (Freund, Gieseke & Nagerl, 1975) that the conditions necessary for proton migration and subsequent defect formation in brucite phases will be realized more easily for surface OH^- ions, due to large mean vibration amplitudes and possible deviations of the OH bonds from the z axis. In high-surface-area materials, such as the $Ni(OH)_2$ sample in this study, a high percentage of the OH^- ions will be close to crystallite surfaces, and a highly defective structure might result. For $Ni(OH)_2$, it seems feasible that the influence of the surface could, in fact, penetrate into the crystal to some extent *via* cooperative displacements due to the short H–H distance.

We thank SERC for providing funds and a CASE Award (to MAT) in conjunction with Inco Alloy Products. The provision of neutron diffraction facilities and technical assistance by ILL is gratefully acknowledged.

References

BRINDLEY, G. W. & CHIH-CHUN KAO (1984). *Phys. Chem. Miner.* **10**, 187–191.

BUSING, W. R. & LEVY, H. A. (1957). *J. Chem. Phys.* **26**, 563–568.

BUSING, W. R. & LEVY, H. A. (1964). *Acta Cryst.* **17**, 142–146.

CHAIX-PLUCHERY, O., BOUILLOT, J., CIOSMAK, D., NIEPCE, J. C. & FREUND, F. (1983). *J. Solid State Chem.* **50**, 247–255.

CHAIX-PLUCHERY, O., CIOSMAK, D., NIEPCE, J. C. & PEYRARD, M. (1984). *J. Solid State Chem.* **53**, 273–276.

FALK, S. U. & SALKIND, A. J. (1969). *Alkaline Storage Batteries.* New York: John Wiley.

FREUND, F., GIESEKE, W. & NAGERL, H. (1975). *Reaction Kinetics in Heterogeneous Chemical Systems*, edited by P. BARRETT, pp. 258–277. Amsterdam: Elsevier.

GREAVES, C. (1985). *J. Appl. Cryst.* **18**, 48-50.
GREAVES, C., THOMAS, M. A. & TURNER, M. (1983). *Power Sources*, **9**, 163-182.
HEWAT, A. W. (1979). *Acta Cryst.* A**35**, 248.
HEWAT, A. W. & BAILEY, I. (1976). *Nucl. Instrum. Methods*, **137**, 463-471.
JOHNSON, C. K. (1965). *ORTEP*. Report ORNL-3794, Oak Ridge National Laboratory, Tennessee.
KOBER, F. P. (1965). *J. Electrochem. Soc.* **112**, 1064-1067.
KOBER, F. P. (1967). *J. Electrochem. Soc.* **114**, 215-218.
MCEWEN, R. S. (1971). *J. Phys. Chem.* **75**, 1782-1789.
OLIVA, P., LEONARDI, J., LAURENT, J. F., DELMAS, C., BRACONNIER, J. J., FIGLARZ, M., FIEVET, F. & DE GUIBERT, A. (1982). *J. Power Sources*, **8**, 229-255.
PETERSON, R. C., HILL, R. J. & GIBBS, G. V. (1979). *Can. Mineral.* **17**, 703-711.
RIETVELD, H. M. (1967). *Acta Cryst.* **22**, 151-152.
RIETVELD, H. M. (1969). *J. Appl. Cryst.* **2**, 65-71.
SAKASHITA, M. & SATO, N. (1973). *Bull. Chem. Soc. Jpn*, **46**, 1983-1987.
SZYTULA, A., MURASIK, A. & BALANDA, M. (1971). *Phys. Status Solidi B*, **43**, 125-128.
TUOMI, D. (1965). *J. Electrochem. Soc.* **112**, 1-12.
WENGELER, H., MARTENS, R. & FREUND, F. (1980). *Ber. Bunsenges. Phys. Chem.* **84**, 873-880.
YOUNG, R. A. & WILES, D. B. (1982). *J. Appl. Cryst.* **15**, 430-438.
ZIGAN, F. & ROTHBAUER, R. (1967). *Neues Jahrb. Mineral. Monatsh.* pp. 137-143.

Acta Cryst. (1986). B**42**, 55-58

Cuboctahedral Anion Clusters in Fluorite-Related Superstructures: Geometrical Calculations

BY D. J. M. BEVAN* AND S. E. LAWTON

School of Physical Sciences, The Flinders University of South Australia, Bedford Park, South Australia 5042, *Australia*

(*Received* 6 *March* 1985; *accepted* 23 *July* 1985)

Abstract

The known structures of $Na_7Zr_6F_{31}$, KY_3F_{10} and tveitite ($Ca_{14}Y_5F_{43}$) have been modelled with clusters of six octahedrally arranged, cation-centred, Archimedian square antiprisms which share corners to generate a cuboctahedral cavity at the centre. This cluster, M_6X_{36}, has point symmetry $m3m$. The anion coordinates calculated from these polyhedral models are compared with observed values derived from X-ray data. Overall the polyhedral models are considered to be good approximations to the real structures.

Introduction

Aléonard, Le Fur, Pontonnier, Gorius & Roux (1978) first discussed the so-called fluorite-related structures of certain mixed alkali and rare-earth fluorides as a group. They defined 'fluorite-related' rather generally to mean the existence in a structure of layers of close-packed cations stacked one upon the other in no particular sequence: in fluorite itself, of course, the stacking sequence is *ABC*. It was clear from their work that a fundamental step in going from the fluorite structure to many superstructures was the conversion of MX_8 cubes to square antiprisms, six of which then shared edges to enclose an X_8 cube, just as six MX_8 cubes do in fluorite itself; both types of isolated cluster have contents M_6X_{32}.

Bevan, Greis & Strähle (1980) proposed another structural principle for *strictly* fluorite-related superstructures (in the sense that the close-packed layer stacking sequence is always *ABC*) in which six MX_8 square antiprisms share *corners* to generate an enclosed X_{12} cuboctahedron, giving rise to a cluster M_6X_{36} (or M_6X_{37} if an additional anion occupies the cavity within the cuboctahedron). Their paper contains photographs of polyhedral models of two known structures, $Na_7Zr_6F_{31}$ (Burns, Ellison & Levy, 1968) and tveitite, $Ca_{14}Y_5F_{43}$ (Bevan, Strähle & Greis, 1982). We were interested to determine just how well such models describe the actual structures, and to this end we have calculated anion coordinates from the models for comparison with those obtained experimentally. Only three structures are discussed here, $Na_7Zr_6F_{31}$, tveitite and KY_3F_{10} (Pierce & Hong, 1973), but the method is generally applicable.

$Na_7Zr_6F_{31}$

This compound is rhombohedral, space group $R\bar{3}$, with hexagonal unit-cell dimensions $a = 14{\cdot}1561\ (7)$, $c = 9{\cdot}579\ (7)$ Å. The relationship of this cell to that of the fluorite structure is given by

$$\begin{pmatrix} a_h \\ b_h \\ c_h \end{pmatrix} = \begin{pmatrix} 2{\cdot}00 & -1{\cdot}50 & -0{\cdot}50 \\ -0.50 & 2.00 & -1.50 \\ 1.00 & 1.00 & 1.00 \end{pmatrix} \begin{pmatrix} a_F \\ b_F \\ c_F \end{pmatrix}. \quad (1)$$

Zr_6F_{37} clusters are centred on lattice points, and each ZrF_8 square antiprism in a cluster shares one edge

* To whom all correspondence should be addressed.

0108-7681/86/010055-04$01.50